CROATICA CHEMICA ACTA CCACAA **65** (2) 367–377 (1992)

ISSN 0011-1643
UDC 541.1
CCA-2065 *Original Scientific Paper*

Non-Equilibrium Behavior in Egg Phosphatidylcholine-Bile Salt Mixed Aqueous Colloids

*Rex P. Hjelm, Jr.**

Los Alamos Neutron Scattering Center, Los Alamos National Laboratory
Los Alamos, New Mexico 87545, USA

Jess Wilcoxon

Organization 1153, Sandia National Laboratory, Albuquerque, NM USA

P. Thiyagarajan

Intense Neutron Source and Chemistry Divisions, Argonne National Laboratory
Argonne, Il. 60436, USA

and

Hayat Alkan

Department Pharmaceutics, University of Illinois,
Chicago, Il. 60680, USA

Received November 29, 1991

Aqueous mixed colloids of bile salt and phosphatidylcholine have particle morphologies that are highly dependent on total lipid concentration. Starting at the highest concentrations globular mixed micelles are found. These elongate into rods with dilution, and then transform into vesicles at the lowest lipid concentrations. Little is known of the mechanism of these concentration-dependent transformations. Here, we report observations from static and dynamic light scattering on egg phosphatidylcholine-glycocholate mixtures, showing that the system passes through a series of large structures upon dilution. As the mixed colloid is diluted to concentrations close to or at the vesicle transition, a well defined structure is formed initially, which is likely to be an aggregate of mixed micelles. This structure then undergoes a series of transformations. The discovery of this structure could be an important clue in understanding the transition from rod-like to vesicle forms.

* Send correspondence to: Rex P. Hjelm, Jr. H805, Los Alamos National Laboratory, Los Alamos, New Mexico 87545. E-MAIL HJELM@GEM.LANL.GOV, HJELM@LANSCE.LANL.GOV

INTRODUCTION

Aqueous mixtures of bile salts and phophatidylcholine are used extensively as models of the structure of bile.[1] Bile is responsible for the solubilization of lipophilic products of the liver, mainly cholesterol. It is, thus, essential in the transport of these materials from the liver through the bile duct and into the gall bladder, where the bile is concentrated and stored until released into the upper intestine in response to hormonal stimulus that occurs because of eating. Once in the upper intestine, bile serves a dual role in further transport of liver lipids and emulsifying ingested fats. The particles present in the mixture aid in the action of lipases, enzymes that catalyze the reactions of lipid digestion, and in the adsorption of the lipid hydrolysates and in the recycled liver products through the intestinal wall.

Bile is a complex mixture of fatty materials and detergents.[2,3] The fats are mainly glycerol phosphates (components of cell membranes) and cholesterol. The detergents are bile salts. There are several types. Each differs by the number and position of hydroxy groups on the cholesterol core of the molecules and by whether or not they are conjugated with glycine or taurine. Other components are present, such as the bile pigments and proteins, but these will not concern us here.

Now, the biological question is: What is the structure of the particles found in these colloids, and how does this relate to the physiological function? To understand this, there are underlying physicochemical principals that must be discovered. These include understanding the structure of the particles and the determinants of self assembly. Of course, these issues are important in their own right.

Considerable effort has gone toward understanding the physical chemistry of this system. The first notable work on the molecular level was that of Small *et al.*,[4] who used polarization microscopy and X-ray diffraction to characterize the phases of a model cholic acid-phospatidylcholine-water system. They identified an isotropic phase in dilute preparations with sufficient cholic acid present to prevent the lecithin from self-assembling into hexagonal or lamellar phases. More details of particle morphology in the isotropic phase(s) resulted from measurements using dynamic light scattering (DLS)[5-8] and nuclear magnetic resonance (NMR).[9] These showed that there is one region of the isotropic phase map that contains mixed micelles of phophatidylcholine and bile salt. The mixed micelles showed the unusual characteristic of increasing in size with decreasing lipid concentration. The measurements showed that particle growth does not continue indefinitely with dilution, but at some point a concentration-induced transition to mixed vesicles and/or sheets occurs.

The mechanism by which these systems transform is not only of significant interest in understanding mixed colloids, but also relates to the physiological functions of bile. As outlined above, bile is concentrated then diluted because of its storage in the gall bladder and subsequent release into the intestine. Thus the evolution of form and mechanism of transformation could give a better understanding of its role in physiological processes.

Our work on egg phosphatidylcholine-glycocholate aqueous mixtures, using small-angle neutron scattering (SANS), has given further detail of the molecular structures in these systems.[10-12] Specifically, we have shown that in the mixed micelle phase, the particles are globular at the highest lipid concentrations and that, as concentration is lowered, the particles elongate and become rod-like. Upon dilution the rod-like particles grow in length. The radius of the rods appears to be the same at the total lipid

concentrations and molar ratios of lecithin to bile salt at which they are present. At high dilutions a concentration-induced transition to single bilayer vesicles occurs. These become smaller with further dilution.

Particle sizes in these systems are considerably larger than the length scales accessible with most SANS instrumentation for the rod-like micelles as one approaches the region where the concentration induced transition to vesicles occurs. However, the important changes occur at length scales accessible with static and dynamic light scattering. Indeed, much of the work on this system in the past few years has involved DLS.[5-8] However, those measurements were done almost entirely at a single angle, 90°; thus the particle shapes and polydispersity could not be completely characterized from these data. Further, little attention was paid to the changes in the system with time. In most instances measurements were started 48 hours after dilution, even though it was known that the system changed during this period. Clearly, there may be important clues in understanding the transitions of these systems in looking at the early time-dependence of this system. We find that the system undergoes continuous and profound changes in structure that were not observed with SANS[10-12] and the earlier DLS[5-8] studies. Light scattering observations at early times provide some definite clues about the mechanisms by which the system transforms on dilution.

EXPERIMENTAL

Materials:

Samples of egg phosphatidylcholine and glycocholate were prepared as described previously[10-12] at molar ratios phosphatidylcholine to bile salt, $\Gamma = 0.8$. All solvents were filtered twice through a 0.2 μ filter to remove dust. The samples were prepared at a total lipid concentration of 50 g/l in buffer, then diluted with buffer to the final concentrations. The diluted samples were filtered twice again. These are then incubated for different times at 22 °C in the dark.

Light Scattering:

Static light scattering (SLS) and dynamic light scattering (DLS) were done using laser light at 633 and 336 nm. The instrumental setup used is described elsewhere.[13] Data were taken at logarithmically-spaced intervals from 11° to 140° for static measurements and 15° and 140° for dynamic measurements. The diffusion coefficients were calculated by fitting the autocorrelation function to a single exponential decay, $C(t) = A\exp(-2Q^2D_{app}t) + B$, where A is the amplitude and B is the incoherent baseline. Here t is time. The momentum transfer, Q, is related to the scattering angle, 2θ, incident wavelength, λ, and index of refraction of the medium, n, by

$$Q = \frac{4\pi n}{\lambda}\sin(\theta)$$

In instances where the diffusion coefficient D_{app} is invariant with Q, the curves are accurately described by exponential decay with a single D_{app}. This suggests a monodispersed population of particles. A strong dependence of D_{app} on Q, in the absence of rotational and internal modes of motion, is taken as indicative of particle polydispersity. In this latter case fitting the curve to a single exponential with a floating base line strongly weights D_{app} to that of the z-average of the particle size distribution.

Since light exposure is a consideration in the samples, multiple scans were sometimes taken at close time intervals, and monitored for changes. No changes were apparent. In addition, samples under inert gas and kept in the dark were set aside and measured once to compare with samples with multiple exposures. The results were very similar. Thus, exposure to light and/or air is not an important issue in the structural changes in these systems.

Data Analysis:

SLS measurements are expressed as the absolute differential cross section per mg total lipid in the sample, $I(Q)/c$ (cm^2mg^{-1}), using toluene as a standard. If the particles in solution are not correlated in position and orientation and $Q < R_{g-1}$, where R_g is the radius of gyration of scattering mass about the particle mass centroid, then the intensity can be approximated by a Gaussian

$$\frac{I(Q)}{c} = \frac{I(0)}{c} \exp\left(-\frac{R_g^2 q^2}{3}\right) \tag{1}$$

The scattering intensity, $I(Q)$, is normalized by the total scattering mass, c, thus $I(0)$ is proportional to the weight average of the particle masses. The measured R_g is the z-average. The domain of Q over which equation (1) applies is called the Guinier regime, and does not depend on details of particle shape.

In cases where the D_{app} is invariant with Q and there are no particle interactions, then D_{app} can be used to calculate an apparent hydrodynamic radius for the particles given by the Stokes-Einstein equation:

$$R_H = \frac{kT}{6\pi\eta D_{app}} \tag{2}$$

where η is the solvent viscosity, k is Boltzmann's constant and T is the absolute temperature.

All values are reported with the rms given in parentheses.

RESULTS

The results of SLS measurements of egg phosphatidylcholine-glycocholate mixtures, $\Gamma = 0.8$, at different total lipid concentrations, are shown in Figure 1. Figure 1A shows data taken at approximately 20 hours after dilution. Figure 1B shows data taken after 5 days. It is seen that the growth of particles on dilution that is observed at intermediate length scales by SANS[10-12] is also apparent at longer length scales. This is implied from the increase in $I(Q)$ with increasing dilution of the mixture that is seen to increase monotonically with dilution both in sample after 20 hours (Figure 1A) and 5 days (Figure 1B) incubation. $I(Q)/c$ for the 16.7 g/l sample (where mixed globular micelles and short rods are found)[12] and that for the 5.0 g/l sample (where vesicles are present)[12] differ by two orders of magnitude.

The shapes of scattering curves also change with dilution in samples incubated for about 20 hours. The data taken for the 16.7 g/l sample (Figure 1A) show a slight upward turn at very low Q that suggests that the Guinier regime has not been accessed in these measurements. This is verified by the Guinier analysis (Figure 2A) that shows a continuous upward curvature. Thus, there are particles in these samples that are larger than the largest $Q^{-1} \approx 2900$ Å accessible in these measurements. As the concentration is decreased, the Q dependence of the scattering becomes stronger, suggesting even larger particle sizes. At 8.3 g/l (Figure 1A) the scattering shows the largest changes at very low Q. Samples at lower total lipid concentrations show progressively flatter scattering curves (Figures 1A) and those at concentration equal to and less than 6.3 g/l show scatter that is Gaussian (Figure 1A). This is verified by the Guinier analysis in Figures 2B and C. The R_g's from these plots are given in Table I. The values cluster around 520 Å and differ by no more than 10%.

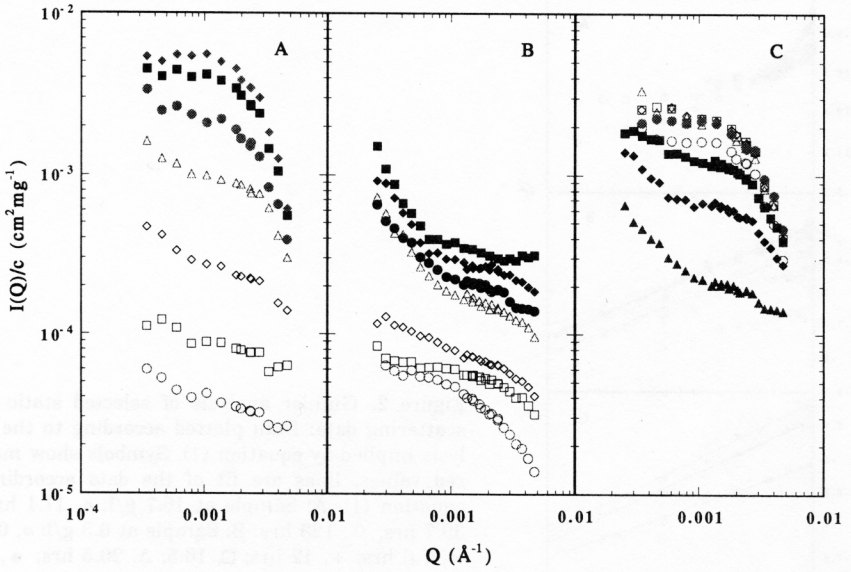

Figure 1. Static light scattering from egg phosphatidylcholine-glycocholate samples as a function of total lipid concentration and time.
A: Samples incubated for approximately 20 hours. o, 16.7 g/l, 7.1 hrs; □, 10.0 g/l, 17.7 hrs; ◇, 8.3 g/l, 18.1 hrs; Δ, 7.1 g/l, 19.7 hrs; ●, 6.3 g/l, 16.5 hrs; ■, 5.6 g/l, 21.2 hrs; ♦, 5.0 g/l 21.7 hrs. B: Samples incubated for approximately 5 days. o, 16.7 g/l, 123 hrs; □, 10.0 g/l, 123 hrs; ◇, 8.3 g/l, 121 hrs; Δ, 7.1 g/l, 119 hrs; ●, 6.3 g/l, 117 hrs; ■, 5.6 g/l, 117 hrs; ♦, 5.0 g/l 118 hrs. ●, C: Samples at 6.3 g/l. o, 0 hrs; □, 7.6 hrs; ◇, 12 hrs; Δ, 16.5 hrs; ●, 20.5 hrs; ■, 46.8 hrs; ♦, 72 hrs; ▲ 117 hrs.

Extended incubation of these samples at room temperature leads to significant changes in the scattering. These are dependent on the total lipid concentration (Figure 1). The changes are the smallest in the most concentrated samples, and become progressively larger in the more dilute samples, particularly as the concentration-dependent transition from rods to vesicles is approached (compare Figures 1A and 1B).

At the highest concentrations studied, the change in the system with time from 17.1 to 123 hours is relatively small. After 123 hours the low-Q region of the curve has increased in intensity, indicating that the system is aggregating into a larger structure. At 10 g/l similar behavior is observed (Figures 1A and B), though in this and all subsequent cases the scattering intensity decreases. At 8.3 g/l the changes are more profound (Figures 1A and B). The scattering intensity drops considerably during the measurements between 18.1 and 121 hours. The size of this change increases as the concentration is lowered further. The form of the final curve is almost identical in each case, reaching a semi-plateau at Q above 0.001 Å^{-1}, then increasing in intensity at lower Q, according to an approximate power law $I \propto Q^{-\alpha}$, where $\alpha \approx 1$. Since we interpret the SANS data at intermediate length scales to be from particles of rod-like geometry[10-12], the SLS data in Figure 1 suggests that these are further associated into arrays of low dimensionality.

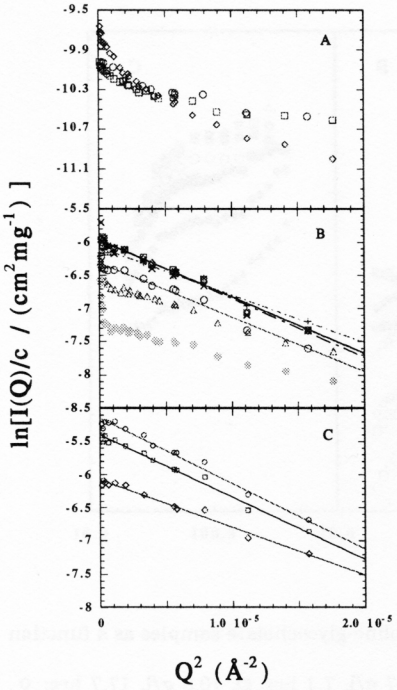

Figure 2. Guinier analysis of selected static light scattering data: Data plotted according to the analysis implied by equation (1). Symbols show measured values, lines are fit of the data according to equation (1). A: Sample at 16.7 g/l: *o*, 17.1 hrs; □, 39.7 hrs; ◇, 123 hrs. B: Sample at 6.3 g/l: *o*, 0 hrs; ×, 7.6 hrs; +, 12 hrs; □, 16.5; Δ, 20.5 hrs; ●, 46.8 hrs. C: Comparison of samples at different dilutions: *o*, 5.0 g/l, 21.7 hrs; □, 5.6 g/l, 21.2 hrs; ◇, 6.3 g/l, 20.5 hrs.

We now present a detailed study of the sequence of events that occur in the 6.3 g/l sample. This is shown in Figure 1C, where the results of measurements from freshly diluted samples are shown as well as measurements after 7.6, 12.0, 16.5, 20.5, 48.6, 72 and 117 hours. There is a continuous change in scattering during this period. The structure remains almost constant for the first 16 hours as verified by a Guinier analysis (Figure 2B). The radii of gyration extracted from this analysis is uniformly 500 (7) Å, there being no significant difference between the measured values (Figure 2B, Table I). The $I(0)$ values from these analyses fall around 0.00256(6) cm^2mg^{-1} for the measurements taken at 7.6, 12.0 and 16.5 hours. The freshly mixed sample does show a significantly lower value of $I(0)$ (Table I). By 20 hours the sample still shows the characteristic Gaussian scattering curve described by equation (1) (Figure 2B), though the value of $I(0)$ has dropped somewhat toward that found in the freshly mixed sample. After two days the scattering has changed to a form midway between that seen earlier and that seen at much later times (Figure 1B). By 3 days the form of the scattering has become like that seen in each final state observed after 5 days, except that the scattering is still somewhat larger than observed at later times.

D_{app} for each sample, as a function of incubation time is shown in Figure 3. The measurement of D_{app} for these samples confirms the observations made with SLS. First, the particle sizes increase with decreasing concentration, as suggested by a decrease in D_{app} (Figure 3A). Second, the size of the particle at a given concentration decreases with incubation time (Figures 3A, B and C). It is also evident from these data that there is a distinct increase in particle polydispersity with incubation, as assessed by the strong Q-dependence of D_{app}.

TABLE I

Radii of gyration, I(0) and hydrodynamic radii of selected samples

[lipid] (g/l)	time (hrs)	R_g (Å)[a]	$I(0)$ (cm^2mg^{-1})[a]	R_H (Å)[b]
6.3	0	496 (8)	0.00182 (4)	578 (19)
6.3	7.6	505 (8)	0.00256 (6)	543 (14)
6.3	12.0	506 (7)	0.00255 (5)	546 (17)
6.3	16.5	516 (13)	0.00258 (10)	548 (14)
6.3	20.5	463 (7)	0.00229 (4)	524 (14)
5.6	21.2	530 (6)	0.00450 (9)	586 (19)
5.0	21.7	544 (8)	0.00581 (14)	585 (36)

[a] From the regression analysis of the Guinier plots in Figure 3.
[b] From D_{app} in Figure 4, using equation (2).

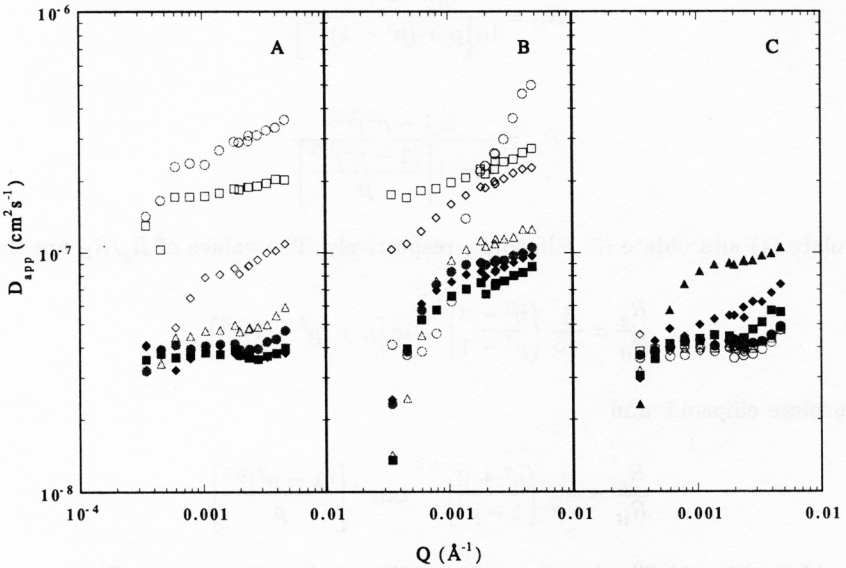

Figure 3. Apparent diffusion coefficients for egg phosphatidylcholine-glycocholate samples as a function of total lipid concentration and time.
A: Samples incubated for approximately 20 hours. o, 16.7 g/l, 7.1 hrs; □, 10.0 g/l, 17.7 hrs; ◇, 8.3 g/l, 18.1 hrs; Δ, 7.1 g/l, 19.7 hrs; ●, 6.3 g/l, 16.5 hrs; ■, 5.6 g/l, 21.2 hrs; ◆, 5.0 g/l 21.7 hrs. B: Samples incubated for approximately 5 days. o, 16.7 g/l, 123 hrs; □, 10.0 g/l, 123 hrs; ◇, 8.3 g/l, 121 hrs; Δ, 7.1 g/l, 119 hrs; ●, 6.3 g/l, 117 hrs; ■, 5.6 g/l, 117 hrs; ◆, 5.0 g/l 118 hrs. ●, C: Samples at 6.3 g/l. o, 0 hrs; □, 7.6 hrs; ◇, 12 hrs; Δ, 16.5 hrs; ●, 20.5 hrs; ■, 46.8 hrs; ◆, 72 hrs; ▲ 117 hrs.

Samples which showed Gaussian scattering in the SLS measurements (Figure 1) (*i.e.*, those at concentrations of 6.3 g/l and less and incubation times of 20 hours and less), also show nearly constant D_{app} with Q. Here we extract a value for R_H using equation (2) (Table I). The values for R_H are close to the values of R_g. The ratios, R_H/R_g are all in the range 0.91 to 0.93.

We can explain this ratio in terms of rigid ellipsoids of revolution with aspect ratio $p = a/b$, where a is the length of the semi-axis coincident with the axis of rotation and b is the semi-axis perpendicular to a. Using this definition $p < 1$ defines an oblate ellipsoid or revolution and $p > 1$ defines a prolate ellipsoid or revolution The radius of gyration for these objects is given as,

$$R_g = b\left(\frac{p^2 + 2}{5}\right)^{1/2} \tag{3}$$

From the expressions of Perrin[14] for the frictional coefficient, f, for ellipsoid of revolution and the fact that $D = kT/f$, we calculate the hydrodymic radius of equation (2) to be

$$R_H = \frac{b(p^2 - 1)^{1/2}}{\ln\left[p + (p^2 - 1)^{1/2}\right]} \tag{4}$$

$$R_H = \frac{b(1 - p^2)^{1/2}}{\tan^{-1}\left[\frac{(1 - p^2)^{1/2}}{p}\right]} \tag{5}$$

for prolate (4) and oblate (5) ellipsoids, respectively. The values of R_g/R_H are then

$$\frac{R_g}{R_H} = \frac{1}{\sqrt{5}}\left(\frac{p^2 + 2}{p^2 - 1}\right)^{1/2} \ln\left[p + (p^2 - 1)^{1/2}\right] \tag{6}$$

for a prolate ellipsoid, and

$$\frac{R_g}{R_H} = \frac{1}{\sqrt{5}}\left(\frac{p^2 + 2}{1 - p^2}\right)^{1/2} \tan^{-1}\left[\frac{(1 - p^2)^{1/2}}{p}\right] \tag{7}$$

for an oblate ellipsoid. The functions (6) and (7) are plotted verses p in Figure 4, where the solution for the observed ratio is also shown. The solutions are at $p \approx 2.6$ and 0.17. The semi-axis are $a \approx 980$ Å and $b \approx 380$ Å for the prolate ellipsoid and $a \approx 130$ Å and $b \approx 790$ Å for the oblate ellipsoid. Analogous calculations for right circular cylinders[15] gives results comparable to that for a prolate ellipsoid. The values of R_H computed using these values are in excellent agreement with the measured values in Table I.

DISCUSSION

The time-dependent evolution of structures that occurs on dilution of a 50 g/l stock is seen to be dependent on the total lipid concentration in the final diluted solution. The closer the final concentration is to the concentration-induced transition to vesicles, the greater the system changes with time. In samples diluted close to or at the concentration where the rod-vesicle transition occurs (5.0 g/l for samples with $\Gamma = 0.8$)[12] the earliest event is the aggregation of the small (approximately 25 Å in

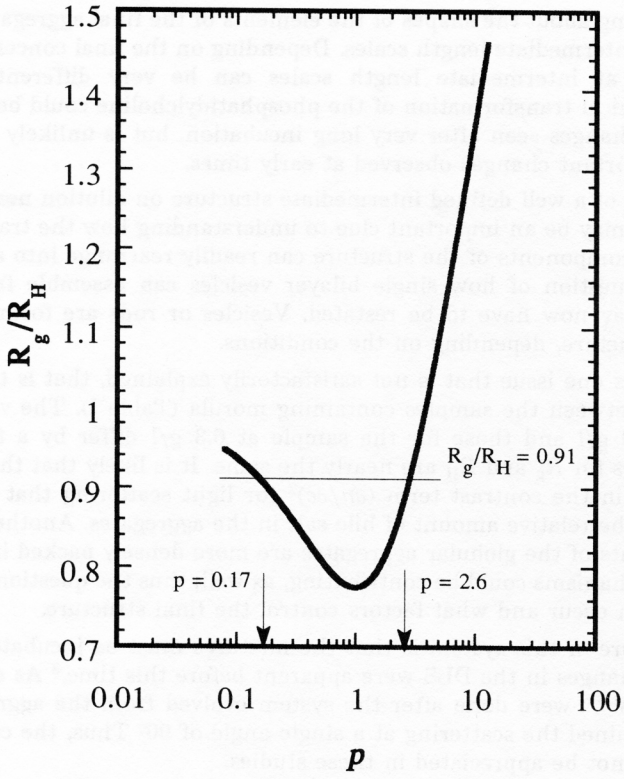

Figure 4. Ratio of radius of gyration to hydrodynamic radius as a function of aspect ratio for ellipsoids of revolution. ——, equations (4) and (5) plotted versed p. Equation (6) applies to the domain $p > 1$; equation (7) to the domain $p < 1$. The two functions are connected by the fact that both equations (6) and (7) have the value $\sqrt{3/5}$ in the limit $p \to 1$. —— corresponds to the measured value R_g/R_H from Table I. Arrows indicate the intersection of the two curves.

radius)[12] globular mixed micelles that are present in the stock solution. The aggregates appear to be of well defined dimensions, as we can calculate the size of equivalent ellipsoids from the data (Table I) and equations (6) and (7). The model used in the calculation is one for which there are analytical expressions for R_g and R_H. Thus, the actual shape is not to be taken literally. A more spherical object with an involuted surface might be devised that would fit the data as well. So we will term this a *globular aggregate*. Polydispersity can also affect this interpretation, but the relative invariance of D_{app} with Q (Figure 3) suggests that this effect is not large. The formation of the globular aggregate likely results from the sudden repartitioning of the bile salt into the bulk solvent from the much less soluble phosphatidylcholine.

The globular aggregates clearly are not stable: they evolve into other structures. Our studies on the sample at 6.4 g/l (Figures 1C and 2B), suggest that the globular aggregates are stable for up to 40 hours, after which the system undergoes rearrangement. This is evidenced by the disappearance of Gaussian scattering and its replacement by an approximate $I \sim Q^{-1}$ power law at the lowest Q-values (Figures 1 and 2).

We know something about the shapes of the elements of the final aggregates from our SANS studies at intermediate length scales. Depending on the final concentration, the objects observed at intermediate length scales can be very different – rods or vesicles.[10-12] Chemical transformation of the phosphatidylcholine could be responsible for some of the changes seen after very long incubation, but is unlikely to have any effect on the important changes observed at early times.

The existence of a well defined intermediate structure on dilution near the rod to vesicle transition may be an important clue to understanding how the transformation takes place. The components of the structure can readily rearrange into another configuration. The question of how single bilayer vesicles can assemble from rod-like mixed micelles may now have to be restated. Vesicles or rods are formed from the same starting structure, depending on the conditions.

There remains one issue that is not satisfactorily explained, that is the large differences in $I(0)$ between the samples containing morula (Table I). The value $I(0)$ for the sample at 5.0 g/l and those for the sample at 6.3 g/l differ by a factor of 2.3 whereas the values for R_g and R_H are nearly the same. It is likely that this is a result of the difference in the contrast term $(\partial n/\partial c)^2$ for light scattering that could result from changes in the relative amount of bile salt in the aggregates. Another possibility is that the elements of the globular aggregates are more densely packed in the 5.0 g/l sample. Both mechanisms could be contributing, as well; thus the question now is how does the evolution occur and what factors control the final structure.

Part of the lore of this system is that the mixtures must be incubated for about 48 hours, since changes in the DLS were apparent before this time.[8] As a result, previous DLS studies[1,5-8] were done after the system evolved from the aggregates. This early work determined the scattering at a single angle of 90° Thus, the complexity of the system could not be appreciated in these studies.

Our SANS measurements[10-12] were always done with the first measurements after 48 hours incubation. Thus, the structures observed at intermediate length scales correspond to the elements of the aggregates found at later times. Since we interpret the data on these length scales as due to long rods, about 27 Å in radius, it would be most consistent to say that the light scattering is the result of a network of rods at these later times. It appears that in waiting for 48 hours, some interesting and important information about the formation of these structures has been missed.

Metastability has been noted and documented in the vesicular phase,[8] but this is the first instance where non-equilibrium behavior has been documented in the mixed micelle phase.

REFERENCES

1. N. A. Mazer, P. Schurtenberger, M. C. Carey, R. Preisig, K. Weigand, and W,. Kanzig, *Biochemistry,* **23** (1984) 1994.
2. M. C. Carey, *Lipid Solubilisation in Bile* in T. Northfield, R. Jarawi, and P. Zentler-Munro (Eds.) *Bile Acids in Health and Disease,* Boston, Kluwer 1988, pp. 61-82.
3. D. J. Cabral and D. M. Small, *Physical Chemistry of Bile* in S. G. Sultz, J. G. Forte and B. B. Rauner (Eds), *Handbook of Physiology, The Gastrointestinal System, III, section 4,* Amer. Phys. Soc., Waverly Press 1989, pp. 621-662.
4. D. M. Small, M. C. Bourges, and D. G. Dervichian, *Biochim. Biophys. Acta* **125** (1966) 563.
5. N. A. Mazer, G. B. Benedek, and M. C. Carey, *Biochemistry* **19** (1980) 601.
6. N. A. Mazer and M. C. Carey, *Biochemistry* **22** (1983) 426.

7. N. A. Mazer and P. Schurtenberger, *Proc. Int. Sch. Phys. »Enrico Fermi«* **90** (1985) 587.
8. P. Schurtenberger, N. A. Mazer, and W. Kanzig, *J. Phys. Chem.* **89** (1985) 1042.
9. R. E. Stark, G. J. Gosselin, J. M. Donowan, M. C. Carey, and M. F. Roberts, *Biochemistry* **24** (1985) 5599.
10. R. P. Hjelm, P. Thiyagarajan, and M. H. Alkan, *J. Appl. Cryst.* **21** (1988) 858.
11. R. P. Hjelm, P. Thiyagarajan, and M. H. Alkan, *Mol. Cryst. Liq. Cryst.* **180A** (1990) 155.
12. R. P. Hjelm, P. Thiyagarajan, D. Sivia, P. Lindner, M. H. Alkan, and D. Schwahn, *Progress in Colloid and Polymer Science* **81** (1990) 225.
13. J. P. Wilcoxon, *J. Phys. Chem.* **94** (1990) 7588.
14. F. Perrin, *Phys. Rad.* **7** (1936) 1.
15. J. G. De La Torre and V. A. Bloomfield, *Qart. Rev. Biophys.* **14** (1981) 81.

SAŽETAK

Neravnotežno ponašanje miješanih koloida fosfatidilkolina iz jajeta i soli žučne kiseline u vodi

R. P. Hjelm, Jr., J. Wilcoxon, P. Thiyagarajan i H. Alkan

Morfologija čestica miješanih koloida žučne kiseline i fosfatidilkolina u vodi vrlo je ovisna o ukupnoj koncentraciji lipida. Pri visokim koncentracijama nađene su globularne miješane micele, koje se s razrjeđenjem elongiraju u štapiće, a zatim se, pri najnižim koncentracijama lipida transformiraju u vezikule. Malo je poznato o mehanizmu tih koncentracijski ovisnih transformacija. Ovdje opisana zapažanja statičkog i dinamičkog raspršenja svjetla na smjesama fosfatidilkolina iz jajeta i glikokolata pokazuju da pri razrjeđivanju sistem prolazi kroz niz velikih struktura. Budući da je miješani koloid bio razrjeđivan do koncentracija koje su blizu ili upravo kod prijelaza vezikula, nastaje dobro definirana struktura za koju se može smatrati da je agregat miješanih micela. Ta struktura tada podliježe nizu transformacija. Otkriće takve strukture može biti važan putokaz za razumijevanje prijelaza iz štapićastih u vezikularne oblike.